Chest CT Findings in Patients With Coronavirus Disease 2019 and Its Relationship With Clinical Features

Jiong Wu, MS, Xiaojia Wu, MS,† Wenbing Zeng, MS,* Dajing Guo, MD,† Zheng Fang, MS,† Linli Chen, MS,† Huizhe Huang, MD,‡ and Chuanming Li, MD†*

Objectives: The aim of this study was to investigate the chest computed tomography (CT) findings in patients with confirmed coronavirus disease 2019 (COVID-19) and to evaluate its relationship with clinical features.

Materials and Methods: Study sample consisted of 80 patients diagnosed as COVID-19 from January to February 2020. The chest CT images and clinical data were reviewed, and the relationship between them was analyzed.

Results: Totally, 80 patients diagnosed with COVID-19 were included. With regards to the clinical manifestations, 58 (73%) of the 80 patients had cough, and 61 (76%) of the 80 patients had high temperature levels. The most frequent CT abnormalities observed were ground glass opacity (73/80 cases, 91%), consolidation (50/80 cases, 63%), and interlobular septal thickening (47/80, 59%). Most of the lesions were multiple, with an average of 12 ± 6 lung segments involved. The most common involved lung segments were the dorsal segment of the right lower lobe (69/80, 86%), the posterior basal segment of the right lower lobe (68/80, 85%), the lateral basal segment of the right lower lobe (64/80, 80%), the dorsal segment of the left lower lobe (61/80, 76%), and the posterior basal segment of the left lower lobe (65/80, 81%). The average pulmonary inflammation index value was (34% ± 20%) for all the patients. Correlation analysis showed that the pulmonary inflammation index value was significantly correlated with the values of lymphocyte count, monocyte count, C-reactive protein, procalcitonin, days from illness onset, and body temperature ($P < 0.05$).

Conclusions: The common chest CT findings of COVID-19 are multiple ground glass opacity, consolidation, and interlobular septal thickening in both lungs, which are mostly distributed under the pleura. There are significant correlations between the degree of pulmonary inflammation and the main clinical symptoms and laboratory results. Computed tomography plays an important role in the diagnosis and evaluation of this emerging global health emergency.

Key Words: SARS-CoV-2, COVID-19, infection, pneumonia, chest CT

(*Invest Radiol* 2020;55: 257–261)

Since the middle of December 2019, many cases of pneumonia with unidentified causes have been found in some hospitals in Wuhan City, Hubei Province, China.[1] At first, it was reported that a number of patients had certain contact with a large seafood and animal market, which suggested an animal-to-human transmission. Soon afterwards, an increasing number of patients without being exposed to the animal market started to grow exponetially, indicating a fact of human-to-human transmission. At present, this kind of pneumonia has been confirmed as a new type of acute respiratory infectious disease caused by coronavirus infection.[2,3] However, it is not clear how expeditiously and sustainably the virus spreads from person to person. On February 12, 2020, the International Committee on Taxonomy of Viruses announced that the official classification of the new coronavirus was severe acute respiratory syndrome coronavirus 2 (SARS-CoV-2). The same day, the World Health Organization announced that the official name of the disease caused by the virus was coronavirus disease 2019 (COVID-19). The coronavirus has been spreading rapidly around the world, infecting no fewer than 70,000 people and leading to a certain degree of public panic.[4–6] On January 30, 2020, the International Health Regulations Emergency Committee of the World Health Organization declared the outbreak a "public health emergency of international concernexternal icon." The epidemic caused by the new coronavirus has become a public health emergency of international concern.

The SARS-CoV-2 is a new strain of coronavirus, which has never been found in human body before. Common clinical symptoms of patients infected with SARS-CoV-2 include fever fatigue and dry cough. Besides, a small number of patients could have nasal congestion, runny nose, sore throat, or diarrhea. Furthermore, in some aggravated cases, infection has led to severe acute respiratory syndrome, renal failure, and even death. In severe cases, patients present with dyspnea and/or hypoxemia 1 week after the onset of the disease, and develop rapidly into acute respiratory distress syndrome, septic shock, metabolic acidosis, and coagulation dysfunction, which are hard to correct. Up to the present, there are only limited data available regarding the typical chest CT imaging findings in COVID-19. In this study, we retrospectively evaluated the chest CT findings in 80 patients with confirmed COVID-19 and evaluate their relationship with the clinical features.

MATERIALS AND METHODS

Patients

The present study sample consisted of 80 patients who had been diagnosed as COVID-19 in our hospitals (outside of the Wuhan area) from January to February 2020. This study received ethics committee approval from our institution, and the committees waived the need for individual consent due to the retrospective nature of the study. The inclusion criteria were (1) epidemiological history—either travel/residence history in Wuhan or exposure history to fevered patients from Wuhan suffering from respiratory symptoms within 14 days before the onset of illness and (2) laboratory diagnosis (real-time fluorescence polymerase chain reaction revealed positive detection of SARS-CoV-2 in throat swabs or lower respiratory tract; the virus gene sequencing of respiratory or blood samples is highly homologous with the known SARS-CoV-2). All the patients underwent thin-section CT at least one time. The exclusion criteria were another confirmed concomitant pulmonary pneumonia or coronavirus infection. Children and pregnant women were also excluded from this study.

Clinical and laboratorial data were obtained from a detailed medical records collected respectively in standardized form by 2 radiologists with 10 and 8 years' experience. The following clinical data of the patients were assessed: sex, age, cough, expectoration, chest pain, muscle ache, abdominal pain or diarrhea, pharyngeal discomfort, dyspnea, dizziness or headache, blood in sputum, and presence of comorbidities

Received for publication February 12, 2020; and accepted for publication, after revision, February 19, 2020.

From the *Department of Radiology, Chongqing Three Gorges Central Hospital; †Department of Radiology, and ‡Office of Academic Research, The Second Affiliated Hospital of Chongqing Medical University, Chongqing, China.

Conflicts of interest and sources of funding: none declared.

This work is funded by the Natural Science Foundation of China (31771619).

Jiong Wu and Xiaojia Wu contributed equally to this work.

Correspondence to: Chuanming Li, MD, Department of Radiology, The Second Affiliated Hospital of Chongqing Medical University, No. 74 Linjiang Rd, Yuzhong District, Chongqing, 400010, China. E-mail: lichuanming@hospital.cqmu.edu.cn.

ISSN: 0020-9996/20/5505–0257

DOI: 10.1097/RLI.0000000000000670

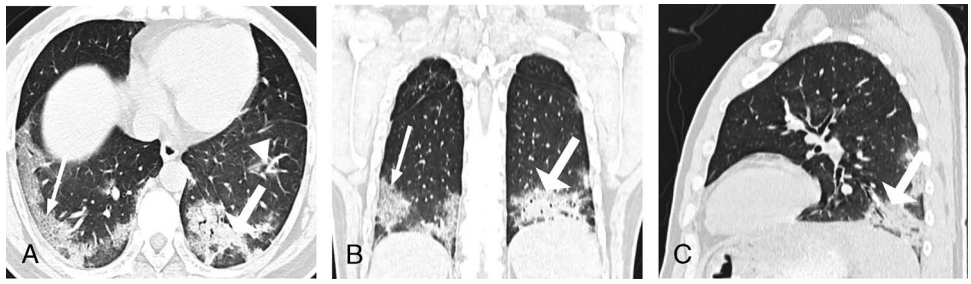

FIGURE 1. A–C, Chest CT of a 38-year-old man. The clinical manifestations were fever (38 C), cough, expectoration, muscle pain, and dyspnea. C-reactive protein and procalcitonin levels were increased. Ground glass opacity (GGO) (white triangle), consolidation (white thick arrow), and interlobular septal thickening (white thin arrow) distributed under the pleura were seen. Nine lung segments including the lateral basal segment, posterior basal segment, posterior basal segment, anterior basal segment of the both lower lobe, and the dorsal segment of the left inferior lobe were involved. In 3 segments, the lesions occupied more than 50% of the total volume. PII = (9 + 3)/40 × 100% = 30%.

(including systemic hypertension, diabetes mellitus, tobacco smoke, asthma, heart disease, chronic obstructive pulmonary disease [COPD], immunodeficiency, and others). Information regarding the physical examination at admission was also evaluated, including the heart rate, body temperature, oxygen saturation, and blood pressure (BP). Moreover, the laboratory data obtained at admission, which included the leukocyte, lymphocyte, neutrophil, monocyte, procalcitonin, and C-reactive protein, were assessed as well. Blood gas analyses were performed in 40 patients whose PH value, $PaCO_2$, and PaO_2 were also assessed. All the blood gas analysis was conducted from arterial blood samples.

CT Scans and Review

The CT examinations were carried out with an 16-row multidetector CT scanner (Siemens Somatom Sensation; Siemens, Erlangen, Germany) using the following parameters: 120 kVp, 150 mA, 1.5 mm collimation, 1.35:1 pitch, sharp kernel (B80f), reconstruction matrix of 512 × 512, slice thickness of 1.0 mm, and high spatial resolution algorithm. All the patients were scanned in a supine position during breath-holding at full inspiration. All CT images were evaluated using a lung window, with a window level of −500 HU and window width of 1500 HU. Two certificated chest radiologists with 10 and 8 years' experience independently reviewed the CT images while they were blinded to the names and clinical data of the patients. The CT imaging features were fully assessed, and the following findings were highlighted: ground glass opacity (GGO), consolidation, interlobular septal thickening, bronchial wall thickening, subpleural line, lymph node enlargement, pleural effusion, and pericardial effusion in accordance with the standard morphologic descriptors based on the Fleischner Society Nomenclature Committee recommendations and similar studies.[7,8] As a rule, a consensus had to be reached between the 2 radiologists about the abnormalities, and discrepancies were reconciled and tackled via discussion. Specifically, the evaluation of the size and extent of lung involvement was based on the segments of the lung anatomy: 10 segments in the right lung and 10 segments in the left lung (2 segments were considered in the apicoposterior segment of the left upper lobe and 2 segments were considered in the inferior front segment of the left lower lobe). According to the evaluation criterion established by Chongqing Radiologist Association of China, the pulmonary inflammation index (PII) was obtained from each patient. PII = (distribution score + size score)/40 × 100% (Fig. 1). Distribution score: scored according to the lesion distribution, one score for each lung segment, and 20 scores for left and right lung. Lesion size was scored according to whether the lesion occupied more than 50% of the lung segment volume, one score for ≥50%, and zero score for <50%. Spearman correlations were performed to evaluate the relationships between the PII value and the clinical symptom and laboratory results of the patients. All statistical analyses were conducted using Statistical Package for Social Sciences software version 23.0 (SPSS Inc, Chicago, IL). *P* values less than 0.05 were considered statistically significant.

RESULTS

Characteristics and Clinical Manifestations

This study included 80 patients diagnosed as COVID-19, of which 42 were male (52%) and 38 were female (48%). All the patients aged 15 to 79 years with an average age of 44 ± 11 years. Twenty-six (33%) of 80 patients were smokers. Sixty-one (76%) of 80 patients

TABLE 1. Characteristics and Clinical Manifestations of the 80 Patients With COVID-19

Characteristics	Patients (n = 80)
Age, y	44 (11)
Sex	
Female	38 (48%)
Male	42 (52%)
Smokers	26 (33%)
Days from illness onset	7 (4)
Comorbidity	15 (18%)
Hypertension	4 (5%)
Diabetes	4 (5%)
COPD	3 (4%)
Immunosuppression	3 (3%)
Heart disease	1 (1%)
Asthma	0 (0%)
Signs and symptoms	
Fever	61 (76%)
Highest temperature	37.80°C (37.30°C–38.20°C)
<37.30°C	19 (24%)
37.30–38.00°C	38 (47%)
38.10–39.00°C	20 (25%)
>39.00°C	3 (4%)
Cough	58 (73%)
Expectoration	11 (14%)
Chest pain	5 (6%)
Muscle ache	13 (16%)
Dyspnea	7 (9%)
Abdominal pain and diarrhea	7 (9%)
Pharyngeal discomfort	9 (11%)
Dizziness and headache	8 (10%)
Blood in sputum	3 (4%)

Data are n (%), n/N (%), and mean (SD), where N is the total number of patients with available data. COVID-19, corona virus disease 2019. COPD, chronic obstructive pulmonary disease.

TABLE 2. Laboratory and Physical Examination Results of the 80 Patients With COVID-19

	Patients (n = 80)
White blood cell count, $\times 10^9$ /L	5.40 (4.20–6.95)
Increased	10 (10%)
Decreased	7 (9%)
Neutrophil count, $\times 10^9$/L	3.74 (2.67–5.20)
Increased	16 (20%)
Decreased	5 (6%)
Lymphocyte count, $\times 10^9$/L	1.15 (0.76–1.40)
Decreased	34 (43%)
Monocyte count, $\times 10^9$/L	0.41 (0.27–0.53)
Increased	8 (10%)
Decreased	1 (1%)
C-reactive protein, mg/L	12.39 (2.71–50.61)
Increased	37 (46%)
Procalcitonin, ng/mL	0.04 (0.03–0.07)
Increased	32 (40%)
Heart rate, beats per minute	88.24 (11.67)
Respiratory rate, breaths per minute	21.05 (3.74)
Systolic pressure, mm Hg	123.46 (14.19)
Diastolic pressure, mm Hg	80.00 (14.04)
SaO_2, % room air	97% (96%–98%)
PH value*	7.45 (0.02)
$PaCO_2$, mm Hg*	39.21 (7.25)
PaO_2, mm Hg*	85.73 (22.11)

Data are n (%), n/N (%), mean (SD), or and median (IQR), where N is the total number of patients with available data. Increasing means exceeding the upper limit of the reference range, and decreasing means being below the lower limit of the reference range.

*Data available for 40 patients.

COVID-19, corona virus disease 2019; SaO_2, arterial oxygen saturation; PH, potential of hydrogen; $PaCO_2$, arterial partial pressure of carbon dioxide; PaO_2, arterial oxygen tension.

had high temperature levels. Fifteen (18%) of 80 patients had comorbidities, 4 (5%) of 80 patients had hypertension, 4 (5%) of 80 patients had diabetes, 3 (4%) of 80 patients had COPD, 3 (3%) of 80 patients had immunosuppression (immunosuppressive drugs taking), and 1 (1%) of 80 patients had heart disease (coronary heart disease). No patients had asthma or other chronic lung disease. With regards to the clinical manifestations, 58 (73%) of 80 patients had cough, 11 (14%) of 80 patients had expectoration, 5 (6%) of 80 patients had chest pain, 13 (16%) of 80 patients had muscle ache, 7 (9%) of 80 patients had abdominal pain or diarrhea, 9 (11%) of 80 patients had pharyngeal discomfort, 8 (10%) of 80 patients had dizziness or headache, 7 (9%) of 80 patients had dyspnea, and 3 (4%) of 80 patients had blood in sputum. On physical examination statistics, the median oxygen saturation was 97% (interquartile rate [IQR], 96%–98%), the average heart rate was 88.24 ± 11.67 bpm, and the respiratory rate was 21.05 ± 3.74 breaths per minute. The average systolic BP was 123.46 ± 14.19 mm Hg, and the diastolic BP was 80.00 ± 14.04mm Hg. Regarding the laboratory data, the median leukocyte count was 5.40 $\times 10^9$/L (IQR, 4.20–6.95 $\times 10^9$/L), lymphocyte count was 1.15 $\times 10^9$/L (IQR, 0.76–1.40 $\times 10^9$/L), monocyte count was 0.41 $\times 10^9$/L (IQR, 0.27–0.53 $\times 10^9$/L), and neutrophil count was 3.74 $\times 10^9$/L (IQR, 2.67–5.20 $\times 10^9$/L), respectively. The median C-reactive protein was 12.39 mg/L (IQR, 2.71–50.60 mg/L), and the procalcitonin was 0.04 ng/mL (IQR, 0.03–0.07 ng/mL). Blood gas analyses were performed in 40 patients. The average PH value was 7.45 ± 0.02, $PaCO_2$ was 39.21 ± 7.25 mm Hg, and PaO_2 was 85.72 ± 22.11 mm Hg. The clinical manifestations and laboratory findings were shown in Tables 1 and 2.

Chest CT Findings

All patients were examined by chest CT 7 ± 4 days after the onset of disease. In chest CT images, 76 (95%) of 80 cases of the patients had abnormalities indicating the pneumonia. The major CT abnormalities observed were GGO (73/80 cases, 91%), consolidation (50/80 cases, 63%), and interlobular septal thickening (47/80, 59%) (Fig. 1). Besides that, 9 (11%) of 80 patients had bronchial wall thickening, 16 (20%) of 80 patients had subpleural line, 5 (6%) of 80 patients had pleural effusion, 3 (4%) of 80 patients had lymph node enlargement, and 4 (5%) of 80 patients had pericardial effusion. The characteristic signs were "crazy paving sign" (23/80, 29%) and "spider web sign" (20/80, 25%) (Figs. 2, 3). The "crazy paving pattern" was characterized by the reticular interlobular septa thickening within the patchy GGO, which had been reported in severe acute respiratory syndrome (SARS) literatures.[9,10] The "spider web sign" was the first time we found and named it. It showed a triangular or angular GGO under the pleura with the internal interlobular septa thickened like a net. The adjacent pleura were pulled and formed a spider web–like shape in the corner. Most of the lesions were multiple, with an average of 12 ± 6 lung segments involved. The lesions showed subpleural distribution in 42 (53%) of 80 cases, diffuse distribution in 7 (9%) of 80 cases, peribronchial distribution in 3 (4%) of 80 cases, and mixed distribution in 24 (30%) of 80 cases. The most common involved lung segments were the dorsal segment of the right lower lobe (69/80, 86%), the posterior basal segment of the right lower lobe (68/80, 85%), the lateral basal segment of the right lower lobe (64/80, 80%), the dorsal segment of the left lower lobe (61/80, 76%), and the posterior basal segment of the left lower lobe (65/80, 81%). The average PII value was (34% ± 20%) for all the patients. Correlation analysis showed that the PII value was significantly correlated with the values of lymphocyte count, monocyte count, C-reactive protein, procalcitonin, days from illness onset, and body

FIGURE 2. A–C, Chest CT of a 60-year-old man. The clinical manifestations were fever (37.8°C), cough, expectoration, and dyspnea. Neutrophil count, lymphocyte count, and C-reactive protein levels were increased. "Crazy paving signs" (white thin arrow) were seen.

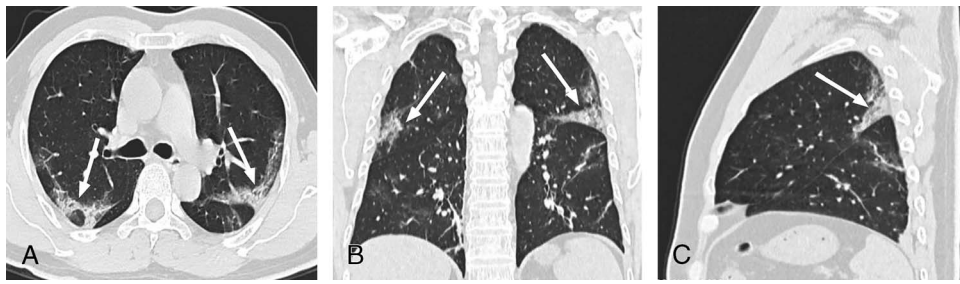

FIGURE 3. A–C, Chest CT of a 44-year-old man. The clinical manifestations were fever (38.5°C), cough, dizziness, and headache. C-reactive protein level was increased. "Spider web signs" (white thin arrow) were seen.

temperature (continuous variable) ($P < 0.05$). The correlation coefficient values were −0.260, −0.258, 0.373, 0.273, 0.287, and 0.544, respectively. The chest CT findings of the patients were shown in Table 3.

DISCUSSION

COVID-19, which is primarily transmitted by contact between people and droplets, turns out to be a new disease of human beings. Whether the novel coronavirus can spread in other ways is unclear, although it could be detected in nasopharyngeal swabs, sputum, lower respiratory secretions, blood, feces, and other samples. Early identification and early intervention are vital to reduce the incidence and mortality of severe cases. In this study, most patients were adults, and there was no significant difference between the numbers of either male or female. Cough and fever were the most common clinical symptoms. The incidence of expectoration, chest pain, muscle ache, abdominal pain or diarrhea, pharyngeal discomfort, headache or dizziness, and dyspnea were less common. This is similar to other types of coronavirus infections such as the SARS and Middle East respiratory syndrome (MERS).[11–13] This implies that they can presumably be classified as the same kind of infection and the target cells of SARS-CoV-2 may also be located in the lower respiratory tract.

For chest CT, 76 cases (95%) had abnormalities indicating the pneumonia. On the whole, in comparison with other types of pneumonia, COVID-19 seemed to cause milder symptoms and severer pulmonary changes on CT. Most of the patients had mild symptoms and mild temperature rise, but their lung manifestations were serious. Multiple lesions were found in multiple segments and lobes of both lungs, which was different from the bacterial pneumonia. In other words, multiple and large lesions of 2 lungs involved simultaneously is not generally spotted in the typical bacterial pneumonia.[14,15] The most common involved lung segments were the dorsal segment of the right lower lobe, the posterior basal segment of the right lower lobe, the lateral basal segment of the right lower lobe, the dorsal segment of the left lower lobe, and the posterior basal segment of the left lower lobe. There were significant correlations among the degree of pulmonary inflammation and the main clinical symptoms and laboratory results. Our results suggested that chest CT could be used to evaluate the severity of the disease and played an important role in clinical practice. For CT features, GGO was the most common of all the abnormalities, followed by consolidation and interlobular septal thickening. This is consistent with the results of the recently published studies.[16–18] Occasionally, the subpleural line and bronchial wall thickening could be seen, whereas pleura effusion, pericardial effusion, or lymph node enlargement were rare to identify. Some of the GGO was characterized by the reticular interlobular septa thickening, which was called "crazy paving pattern." It resulted from the alveolar edema and interstitial inflammatory of acute lung injury, which had been reported in SARS.[9,10] In another situation, some of the GGO showed a triangular or angular shape under the pleura with the internal interlobular septa thickened like a net. The adjacent pleura were pulled and formed a spider web–like shape in the corner. Thus, we named it "spider web sign." However, the pathological basis needs further pathological confirmation. It is a specific sign for COVID-19, which has not been reported in other diseases in the literature. At present, it is not clear whether it has clinical value in evaluating the prognosis of patients. Recently, Pan et al have analyzed the time course of lung changes in 21 mild patients with confirmed COVID-19. They found that the initial lung manifestation was subpleural GGO, which turned to consolidation 2 weeks after the onset of the disease, and then the lesions were gradually absorbed, leaving a wide range of GGO and subpleural parenchymal bands.[17] In another article, the authors found that after 7 days of treatment for the mild patients, there was a significant reduction in GGO on chest CT. On the 13th day after admission, most of the ground glass disappeared. Our patients constituted

TABLE 3. Chest CT Findings of the 80 Patients With COVID-19

	Patients (n = 80)
CT features	
GGO	73 (91%)
Consolidation	50 (63%)
Interlobular septal thickening	47 (59%)
Crazy paving pattern	23 (29%)
Spider web sign	20 (25%)
Subpleural line	16 (20%)
Bronchial wall thickening	9 (11%)
Lymph node enlargement	3 (4%)
Pericardial effusion	4 (5%)
Pleural effusion	5 (6%)
Lung segment involved	
Average lung segments involved	12 (6)
Dorsal segment of the right lower lobe	69 (86%)
Lateral basal segment of the right lower lobe	64 (80%)
Posterior basal segment of the right lower lobe	68 (85%)
Dorsal segment of the left lower lobe	61 (76%)
Posterior basal segment of the left lower lobe	65 (81%)
PII value	34% (20%)
Distribution	76 (95%)
Subpleural distribution	42 (53%)
Diffuse distribution	7 (9%)
Peribronchial distribution	3 (4%)
Mixed distribution	24 (30%)

Data are n (%), n/N (%), or mean (SD), where N is the total number of patients with available data. CT, computed tomography; COVID-19, corona virus disease 2019; GGO, ground glass opacity; PII, pulmonary inflammation index.

a complete group with mild, severe, and critical types.[19] All patients completed CT examination within 2 days after admission, which was 7 ± 4 days from the onset of the disease.

At present, to our knowledge, all patients have not been examined by pathology in the world, so it is impossible to know the exact pathological manifestations of COVID-19. However, according to the morphological changes of the CT features, pathological manifestations could be speculated although there was no direct evidence. The ground glass density lesions could be caused by the exudation of alveoli. The appearance of consolidation indicated that the alveoli were completely filled by inflammatory exudation. The thickening of interlobular septum indicated that the pulmonary interstitium has been involved. In the late stage of acute respiratory distress syndrome, diffuse alveolar, and interstitium damage may occur.

The COVID-19 needs to be differentiated from other diseases, such as SARS and MERS. They all showed multiple ground glass shadows and solid lesions in both lungs, mainly distributed under the pleura, which were difficult to distinguish.[20–22] However, SARS and MERS had faster disease progress and heavier lung damages than COVID-19 infection did. Likewise, COVID-19 should be distinguished from other kinds of viral pneumonia such as influenza virus, parainfluenza virus, adenovirus, respiratory syncytial virus, rhinovirus, human metapneumovirus, and mycoplasma pneumonia.

In conclusion, in this study, we found that common chest CT findings in COVID-19 include multiple GGO, consolidation, and interlobular septal thickening in both lungs, with mostly subpleural distribution. There were significant correlations among the degree of pulmonary inflammation and the main clinical symptoms and laboratory results. Computed tomography played an important role in the diagnosis and evaluation of this emerging global health emergency. Nevertheless, this study has 3 limitations. First of all, this was a retrospective study involving a small number of patients with proven SARS-CoV-2 infection. Second, none of the patients had a lung biopsy or autopsy to reflect the histopathological changes. Third, this study was a cross-sectional study, and we could not analyze the dynamic CT changes in different stages. In the future work, we will investigate the chest CT features of differential stages of COVID-19 by using larger, more diverse samples.

REFERENCES

1. World Health Organization. Novel coronavirus - China. 2020. Available at: https://www.who.int/csr/don/12-january-2020-novel-coronavirus-china/en/.
2. Chaolin H, Yeming W, Xingwang L, et al. *The lancet*. Published Online January 24, 2020. Available at: https://doi.org/10.1016/S0140-6736(20)30183-5.
3. Huang C, Wang Y, Li X, et al. Clinical features of patients infected with 2019 novel coronavirus in Wuhan, China. *Lancet*. 2020;395:497–506.
4. World Health Organization. Novel coronavirus - Japan (ex-China). 2020. Available at: http://www.who.int/csr/don/17-january-2020-novel-coronavirusjapan-ex-china/en/.
5. World Health Organization. Novel coronavirus - Republic of Korea (ex-China). 2020. Available at: http://www.who.int/csr/don/21-january-2020-novelcoronavirus-republic-of-korea-ex-china/en/.
6. CDC. First travel-related case of 2019 novel coronavirus detected in United States. 2020. Available at: https://www.cdc.gov/media/releases/2020/p0121-novel-coronavirus-travel-case.html.
7. Hansell DM, Bankier AA, MacMahon H, et al. Fleischner society: glossary of terms for thoracic imaging. *Radiology*. 2008;246:697–722.
8. Schoen K, Horvat N, Guerreiro NFC, et al. Spectrum of clinical and radiographic findings in patients with diagnosis of H1N1 and correlation with clinical severity. *BMC Infect Dis*. 2019;19:964.
9. Ketai L, Paul NS, Wong KT. Radiology of severe acute respiratory syndrome (SARS): the emerging pathologic-radiologic correlates of an emerging disease. *J Thorac Imaging*. 2006;21:276–283.
10. Wong KT, Antonio GE, Hui DS, et al. Thin-section CT of severe acute respiratory syndrome: evaluation of 73 patients exposed to or with the disease. *Radiology*. 2003;228:395–400.
11. Lee N, Hui D, Wu A, et al. A major outbreak of severe acute respiratory syndrome in Hong Kong. *N Engl J Med*. 2003;348:1986–1994.
12. Assiri A, Al-Tawfiq JA, Al-Rabeeah AA, et al. Epidemiological, demographic, and clinical characteristics of 47 cases of Middle East respiratory syndrome coronavirus disease from Saudi Arabia: a descriptive study. *Lancet Infect Dis*. 2013;13:752–761.
13. Muller NL, Ooi GC, Khong PL, et al. High-resolution CT findings of severe acute respiratory syndrome at presentation and after admission. *Am J Roentgenol*. 2004;182:39–44.
14. Gharib AM, Stern EJ. Radiology of pneumonia. *Med Clin North Am*. 2001;85:1461–1491, x.
15. Koo HJ, Lim S, Choe J, et al. Radiographic and CT features of viral pneumonia. *Radiographics*. 2018;38:719–739.
16. Song FX, Shi NN, Zhang ZY, et al. Emerging coronavirus 2019-nCoV pneumonia. *Radiology*. 2020;200274:200274.
17. Pan F, Yan TH, Sun P, et al. Time course of lung changes on Chest CT during recovery from 2019 novel coronavirus (COVID-19) pneumonia. *Radiology*. 2020;200370. doi:10.1148/radiol.2020200370.
18. Jeffrey K. Chest CT findings in 2019 novel coronavirus (2019-nCoV) infections from Wuhan, China: key points for the radiologist. *Radiology*. 2020;200241. doi:10.1148/radiol.2020200241.
19. Duan YN, Qin J. Pre- and posttreatment chest CT findings: 2019 novel coronavirus (2019-ncov) pneumonia. *Radiology*. 2020;200323. doi:10.1148/radiol.2020200323.
20. Das KM, Lee EY, Enani MA, et al. CT correlation with outcomes in 15 patients with acute Middle East respiratory syndrome coronavirus. *AJR Am J Roentgenol*. 2015;204:736–742.
21. Ajlan AM, Ahyad RA, Jamjoom LG, et al. Middle East respiratory syndrome coronavirus (MERS-CoV) infection: Chest CT findings. *AJR Am J Roentgenol*. 2014;203:782–787.
22. Hui DS, Memish ZA, Zumla A. Severe acute respiratory syndrome vs. the Middle East respiratory syndrome. *Curr Opin Pulm Med*. 2014;20:233–421.